International Journal of Technology (2015) 4: 622-630
ISSN 2086-9614

OPTIMIZING COUPLING REGION AS SENSING AREA IN OPTICAL RING RESONATOR SENSOR APPLICATIONS

Purnomo Sidi Priambodo[1*], Sasono Rahardjo[2], Gunawan Witjaksono[3], Djoko Hartanto[1]

[1] *Department of Electrical Engineering, Faculty of Engineering, Universitas Indonesia, Kampus Baru UI Depok, Depok 16424, Indonesia*
[2] *Agency for the Assessment and Application of Technology, Jalan M.H. Thamrin 8, Jakarta 10340, Indonesia*
[3] *Malaysian Institute of Microelectronic Systems, MIMOS Berhad, Technology Park Malaysia, Kuala Lumpur 57000, Malaysia*

(Received: June 2015 / Revised: September 2015 / Accepted: October 2015)

ABSTRACT

Optical Ring Resonators (ORR), whether based on fiber optics or an optical micro ring on substrate structures have been studied and explored extensively to be used for optical sensor applications. The outstanding advantage of optical ring resonator structure is its spectral response shape change due to the variations of the refractive index of the surrounding medium, medium loss due to absorption and scattering, and coupling loss between waveguides in the optical ring structure. The change of spectral response due to the variations of optical medium on the optical ring structure is a phenomenon that can be used to sense the optical property change of physical or biological materials. Some developments of Waveguide (WG) ORR sensors are in progress mostly for bio-sensor applications, since it is free from Electromagnetic Interference (EMI) and is non-physically destructive. In this paper, we discuss our research in developing optical bio-sensor in the form of a WG optical ring resonator. The focus of the research is optimizing the coupling region as sensing area to obtain the optimal coupling coefficient for the most sensitive sense. The results show that the variations of coupling coefficient is not linear with respect to the resonant peak output, such that we are able to locate the most sensitive coupling coefficient to sense.

Keywords: Optical bio-sensor; Optical coupling; Optical Ring Resonator; Resonance; Spectral response

1. INTRODUCTION

Optical sensors have been developed for several decades, right after the inventions of laser in 1958 (Schawlow et al., 1958; Maiman, 1960; Hall et al., 1962; Holonyak, Jr. et al., 1962) and fiber optics in 1966 (Kao et al., 1966). A fiber-based optical sensor is very interesting, since it is non-invasive detection. There are at least three parameters that can be used to detect the change surrounding the fiber or optical waveguide. First is the refractive index surrounding the core of the fiber. The second is the optical perturbation surrounding the waveguide, where perturbation can be in the form of scattering and absorption centers. The third is perturbation inside the waveguide itself.

During the years of development, there are many techniques that have been proposed to realize

* Corresponding author's email: pspriambodo@gmail.com, Tel. +62-21-7270078, Fax. +62-21-7270077
Permalink/DOI: http://dx.doi.org/10.14716/ijtech.v6i4.1271

the optical sensors. Some use thin film waveguide structures and others use fiber optics as sensors. There are several techniques available to analyze refractive index variations, either perturbation scattering or absorptive material that exists surrounding the cladding and disturbing evanescent wave in the waveguide sensor (Lieberman et al., 1990; Kim et al., 2011; Boiarski et al., 1995; Zhang et al., 2014). Furthermore, there are some techniques that utilize fiber optics bending which correspond to fiber light scattering, which is due to fiber curvature variations exceeding the critical angle limit. This technique is mainly used in detecting pressure, strain, dislocation and weight (Gong et al., 2011; Gouveia et al., 2011; Zhou et al., 2012; Stupar et al., 2012). Moreover, fiber optic sensors can be realized for temperature sensors (Boiarski et al., 1995; Zhang et al., 2014).

Besides using a single fiber sensor structure, there are other types of optical sensors that utilize the coupling region as the sensing area. The detection technique utilizing the coupling area looks like the one with fiber cladding, i.e. it is manipulating the evanescent wave because of the sensed material refractive index variation in the coupling area between the waveguides. The advantage of using the waveguide coupling structure is that the area of detection is relatively very small and it has a very sensitive sensing capability.

In this paper, we propose to combine optical coupling as a detection area with the optical ring resonator structure to be a sensitive optical sensor device. The optical ring resonator has at least four outstanding output characters. Thus, the four characters are: peak spectral response at resonance condition, narrow linewidth spectral response, maximum to minimum ratio response, which is called Finesse, and the repeating response with respect to wavelength. The first three characters of output spectral response will change if one of the optical detection parameters changes. Thus, it could be the coupling value of optical ring resonator, the absorption and refractive index surrounding the waveguide core and the scattering of light inside the optical ring. The main purpose of implementing an optical ring resonator structure is to improve the detection process, which becomes more sensitive. In this paper, we discuss a theoretical analysis of our recent research in optimizing the coupling region as a sensing area in an optical ring resonator sensor, such that we can evaluate all mandatory parameters to obtain a sensitive optical sensor.

2. METHODOLOGY

In this discussion, the theoretical analysis will be explored in two separate discussions, i.e. waveguide coupling and an optical ring resonator. The sensor structure is shown in Figure 1, or sometimes it is called a Direct-Loop Optical Ring Resonator (DLORR) (Rahardjo et al., 2014).

The ring part in practical application is known as either a Single Mode Polarization-Maintained Fiber (SM-PMF) or a Single Mode Dielectric Rectangular Waveguide (SMDR-WG) on a substrate. If fiber optics are used, the sensor size is relatively large, however, in the opposite condition, if a single mode waveguide on a substrate is used, the sensor size can be relatively smaller and it can be less than 1 cm^2. The reason to implement optical ring resonator is to obtain optical resonance phenomena that make the detection process become more effective and with a higher resolution.

2.1. Waveguide Coupling Analysis

In this theoretical analysis, we used a single mode dielectric rectangular (two-dimensional) WG optical coupler on a substrate as shown on Figure 2. There are some variables influencing the optical detection process. Those are n_1, n_2 and n, which are refractive indices of WG_1, WG_2 and the area surrounding those two WG, respectively. More parameters are related to the distance between the WGs (2a), the wavelength of light λ, the WG thickness d and the coupling area length L_0.

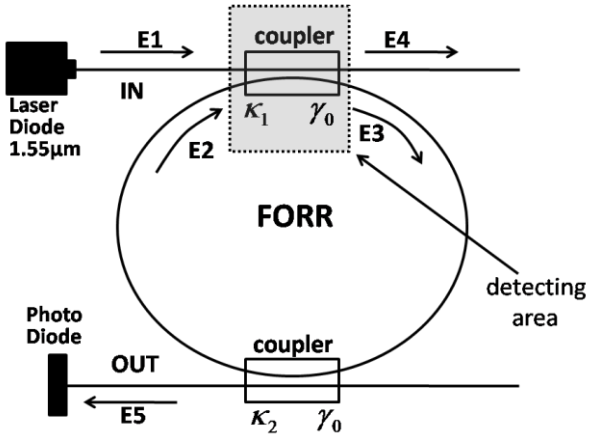

Figure 1 Optical sensor incorporating an optical ring resonator structure with the coupling region as the sensing area. The optical coupling is a Direct-Loop Optical Ring Resonator (DLORR) (Rahardjo et al., 2014)

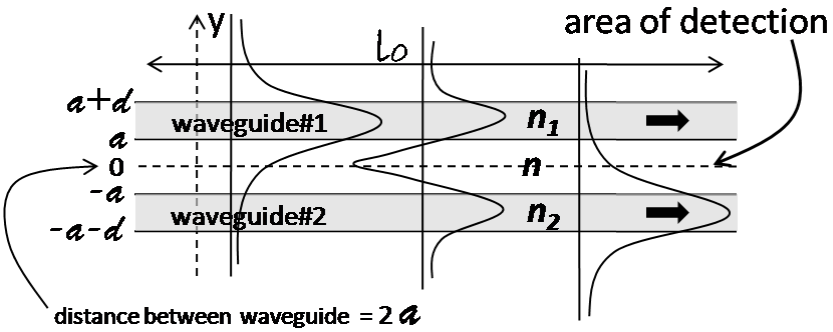

Figure 2 The illustration of a Single Mode Dielectric Rectangular Waveguide (SMDR-WG) coupler on a substrate structure's analysis. For a symmetrical waveguide coupler structure ($n_2 = n_1$) > n, where n varies, due to the variation in the detected medium related to the distance between the WGs (2a), the wavelength of light λ, the WG thickness d and the coupling area length L_0.

The coupling coefficient ς is influenced by optical parameters of the waveguides and surrounding medium as shown on Equation 1 below (Saleh & Teich, 1991) and it is illustrated in Figure 2 above:

$$\varsigma_{2.1} = \tfrac{1}{2}\left(n_2^2 - n^2\right)\frac{k_0^{\,2}}{\beta_1}\int_{a}^{a+d} u_1(y)\,u_2(y)\,dy$$
$$\varsigma_{1.2} = \tfrac{1}{2}\left(n_1^2 - n^2\right)\frac{k_0^{\,2}}{\beta_2}\int_{-a-d}^{-a} u_2(y)\,u_1(y)\,dy \qquad (1)$$

where $\varsigma_{2.1}$ is coupling coefficient from WG 2 to WG 1 and $\varsigma_{1.2}$ is vice versa. $\varsigma_{2.1}$ and $\varsigma_{1.2}$ is equal to ς when the waveguide coupling is symmetric, i.e. $n_2 = n_1$ and of course $\beta_2 = \beta_1$. In general:

$$\varsigma = \left(\varsigma_{1.2}\,\varsigma_{2.1}\right)^{1/2} \qquad (2)$$

From Equation 1 we see that the coupling coefficient ς is mostly determined by the structural design of the waveguide coupler, which is represented by the distance between waveguides 2a

that is fixed, the waveguide refractive index $n_2 = n_1$ that is fixed and the surrounding refractive index n that may vary, due to the variation of the refractive index medium. The variation of the refractive index medium between the two waveguides in the coupler, as shown in Figure 2, will be sensed as a variation of the coupling coefficient ς. The total value of the sensing waveguide coupling (Saleh & Teich, 1991) is defined as κ_1:

$$\kappa_1 = \sin^2 \varsigma L_0 \tag{3}$$

2.2. Resonat Optics Analysis

The Optical Ring Resonator structure is used to improve the optical detection process in a more effective way, thus gaining higher resolution. In this system (as shown on Figure 1), we are interested in the signal from E5, which shows the spectral response variations, which correspond to the coupling value κ_1 variation that is due to the detected refractive index variation in the coupling area. $|E5/E1|^2$, which is derived by setting: κ_1 (as sensing coupling variable) and κ_2 (as a constant), with an equal coupling loss γ_0 and the fact that the relationship between E2 and E3 is formulated as follows (Priambodo et al., 2015):

$$E_2 = E_3 \left(1-\kappa_2\right)^{1/2} \left(1-\gamma_0\right)^{1/2} e^{-\alpha_0 L} e^{j\beta L} \tag{4}$$

hence, $|E5/E1|^2$ can be written as:

$$\left|\frac{E_5}{E_1}\right|^2 = \frac{\left(1-\gamma_0\right)^2 \kappa_1 \kappa_2}{Z} \tag{5}$$

where

$$Z = \left(1-\left(1-\gamma_0\right)\left(1-\kappa_1\right)^{1/2}\left(1-\kappa_2\right)^{1/2} e^{-\alpha_0 L}\right)^2 + 4\left(1-\gamma_0\right)\left(1-\kappa_1\right)^{1/2}\left(1-\kappa_2\right)^{1/2} e^{-\alpha_0 L} \sin^2 \frac{\beta L}{2} \tag{6}$$

α_0 is the fiber optic loss coefficient, L is the length of the fiber ring and β is the fiber optic propagation constant and is formulated as:

$$\beta = n_{eff}\,(2\pi/\lambda) \tag{7}$$

where n_{eff} is the effective refractive index of the fiber.

For Direct-Loop Fiber Optical Ring Resonator (DL-FORR) configuration, at a resonant condition, the phase relationship inside loop is written simply as:

$$\beta L = q2\pi \tag{8}$$

The theoretical output wavelength response profile towards input intensity is shown in Figure 3.

The optical sensor system we discuss here is combining two optical phenomena, i.e: (1) Single Mode Dielectric Rectangular (two-dimensional) WG optical coupler on the substrate as the sensing area and (2) WG Optical Ring Resonator. The combination system transforms the variation of the refractive index medium in the optical coupling area, which is due to the sensed object variation, on to the variation $|E5/E1|^2$ output spectral response. The output spectral response is easily readable and analyzed by Digital Signal Processing (DSP) equipment, which is accurate enough to determine the variation of the sensed objects.

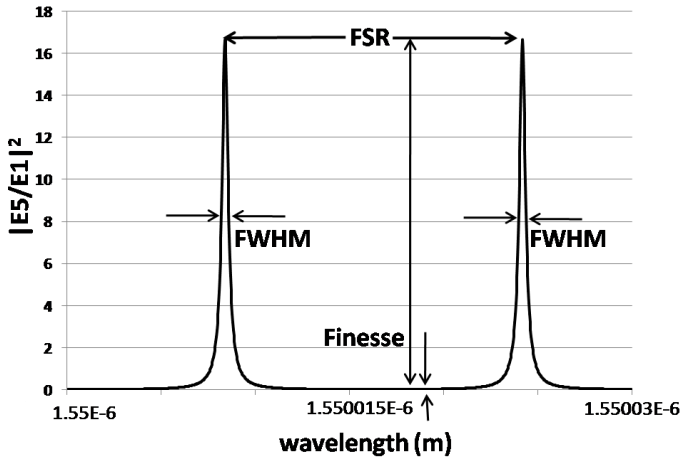

Figure 3 $|E5/E1|^2$ vs wavelength: Resonance Intensity Response Output Profile, where we use typical fiber-optical values of: $\gamma_0 = 0.05$, $\kappa = \kappa_1 = \kappa_2 = 0.1$, $L = 0.1\ m$ and $\alpha_0 = 6.9E-5/m$

The following Figure 4 is a simulation, which gives an illustration of how the variation of coupling κ_1 due to the refractive index variation of the sensed material, will vary with the resonance spectral output response.

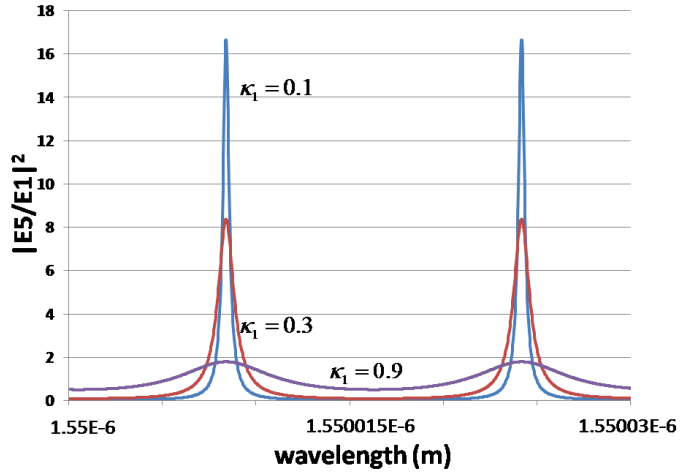

Figure 4 The changes of Resonance Intensity Response Profile$|E5/E1|^2$ vs. wavelength due to varying the coupling coefficient κ_1 at the sensing coupling area

Figure 4 shows very clearly that the change of from 0.1 to 0.9 will change shape of the spectral profile output. The DSP system should help us to analyze the change of the profile shape. The realization of the coupling structure for the sensing area is illustrated in Figure 5 below, where there is a groove channel between WG in the sensing area. The groove is proposed to trap the sensed material to be a coupling medium. A special chemical tag (such used in bio sensing) can be applied for this purpose.

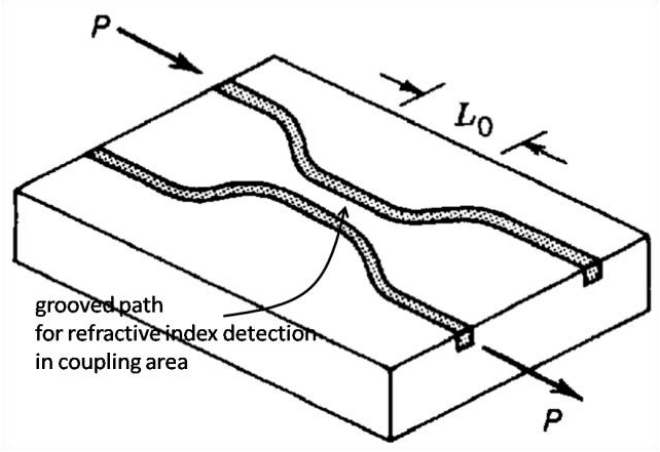

Figure 5 An illustration of a Single Mode Dielectric Rectangular (two-dimensional) WG optical coupler on a substrate for optical sensing area. There should be a grooved path to trap a sensed material as a coupling medium (Saleh et al., 1991)

3. RESULTS AND DISCUSSION

In order to improve the coupling region as the sensing area, that area should be optimized based on the variation of the sensed material and the sensor structure. Figures 3 and 4 show the unique profile of the output spectral response and its variations, due to the varying κ_1 of the optical coupler, which is caused by the variation of the sensed material refractive index *n*. Figure 3 shows that at least four characters may be explored to be parameters of the output sensing indicators. The first is the Full Width Half Maximum (FWHM) and the second is the Free Spectral Range (FSR), where this is due to the Optical Ring Resonator length. The third is the Finesse and the fourth is the peak of $|E5/E1|^2$ at the resonant condition. In this discussion, we are interested in exploring the variation of $|E5/E1|^2$ at the resonant condition as the output of the sensing indicator.

At the resonant condition with respect to κ_1 and at the resonant conditions shown in Equations 5 and 6 can be written as:

$$\left|\frac{E_5}{E_1}\right|^2_{at\ resonance} = \frac{\left(1-\gamma_0\right)^2 \kappa_1\, \kappa_2}{\left(1-\left(1-\gamma_0\right)\left(1-\kappa_1\right)^{1/2}\left(1-\kappa_2\right)^{1/2} e^{-\alpha_0 L}\right)^2} \tag{9}$$

The graph of Figure 6 shows the varying of $|E5/E1|^2$ at the resonant peak with respect to κ_1. The graph shows that in the region between 0.2 and 0.9 is a linear detection regime, for some typical value of: $\gamma_0 = 0.05$, $\kappa_2 = 0.1$ and $\alpha_0 = 6.9E-5/m$. It is good, if the design locates the effect of the sensed material medium, which corresponds to this linear detection. It helps the measurement to be more accurate.

Once the coupling value range is determined, the next step is how to optimize the variables, which determine the coupling value κ_1, i.e. the coupling coefficient between WGs (ς) and the coupling interaction length (L_0). The relationship between κ_1, ς and L_0 is written in Equation 3. This equation shows that κ_1 is determined by ς and L_0. If ς has a large range, then L_0 can be designed as short as possible. Determining L_0 is easier when it can be determined after optimizing ς.

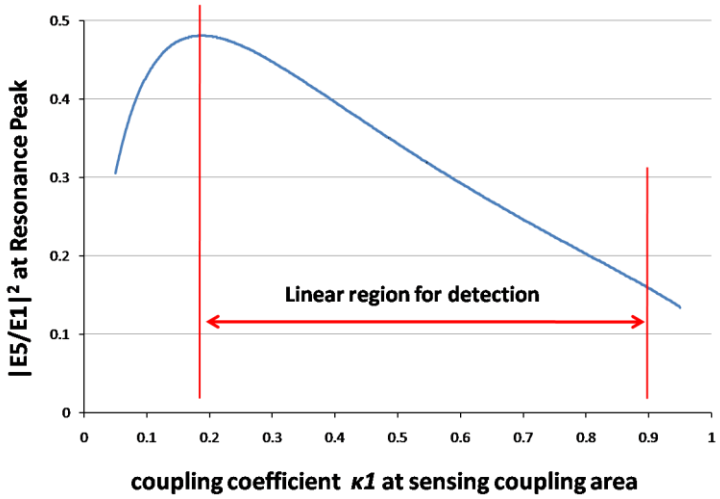

Figure 6 The varying of $|E5/E1|^2$ at the resonant peak with respect to κ_1 (detecting the coupling value)

There are at least two different sensing methods. The first is sensing the availability of sensed material in the detecting area. The second is detecting the variation of refractive index materials. In this research, we are interested in the first case. The sensed refractive index *n* should be known, hence, the coupler structure can be designed to obtain a maximum ς change between existing and non-existing sensed material in the coupling area. Since the sensed material has a material refractive index ranging from 1 (air) to *n*. The maximum ς change can be written as:

$$\Delta\varsigma_{\max} \approx \tfrac{1}{2}\left(n_{sensed}^2 - 1\right)\frac{k_0^{\,2}}{\beta_1}\int_a^{a+d} u_1(y)\,u_2(y)\,dy \tag{10}$$

Equation 10 shows that $\Delta\varsigma_{\max}$ can optimized by the value of the coupler structure which is represented by the integral term $\int_a^{a+d} u_1(y)\,u_2(y)\,dy$. In order to optimize the integral term, the parameters of a (half distance between WGs), *d* (WG thickness) and WG refractive index of $n_1 = n_2$ must be adjusted for the optimum value. Figure 7 shows the relationship between $\Delta\varsigma_{\max}$ and a (half distance between WGs), with typical values of $n_{sensed} = 1.43$, $\lambda = 1550$-nm, d = 750-nm and ***a*** between *200* to *1200-nm*. The graph shows an exponential relationship.

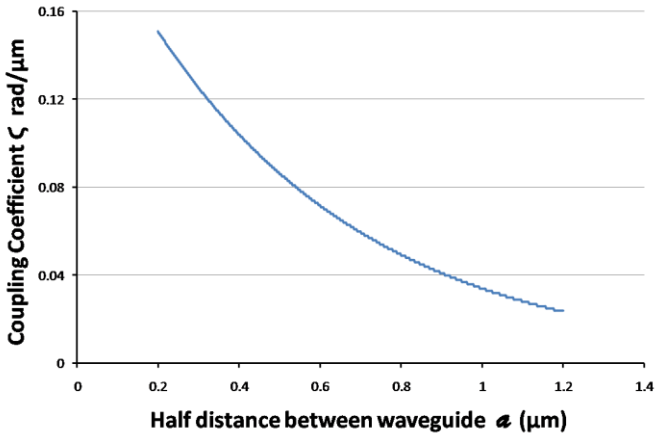

Figure 7 The relationship between $\Delta\varsigma_{\max}$ and a (half distance between WGs)

4. CONCLUSION

We discussed the possibility of an optical coupling region as a sensing area, when the optical coupler is equipped with an optical ring resonator. By incorporating an optical ring resonator, a better outstanding of output resolution can be obtained. The sensing material located in the optical coupler area should be in the form of a varying refractive index. Our theoretical simulation in Figure 6 shows that the output $|E5/E1|^2$ at resonant peak is a function of κ_1, where it shows a linear relationship for κ_1 values between 0.2 and 0.9. Furthermore, the sensed coupling value κ_1, is determined by the interaction length of the coupling area L_0 and the coupling coefficient ς. The maximum ς variation or $\Delta\varsigma_{max}$ can be optimized by designing the coupling interaction as an integral term, such as shown in Equation 10. Figure 6 shows an exponential relationship; as a consequence of obtaining a constant optimum κ_1 value, then the coupling interaction length (L_0) should be extended for exponential purposes, where the sensing area is expanded as well in an exponential way.

5. REFERENCES

Boiarski, A.A., Pilate, G., Fink, T., Nilsson, N., 1995. Temperature Measurement in Power Plant Equipment using Distributed Fiber Optic Sensing. *IEEE Transactions on Power Delivery*, Volume 10(4), pp. 1771–1778

Gong, Y., Zhao, T., Rao, Y.J., Wu, Y., 2011. All-fiber Curvature Sensor based on Multimode Interference. *IEEE Photonics Technology Letters*, Volume 23(11), pp. 679–681

Gouveia, C., Jorge, P.A.S., Baptista, J.M., Frazao, O., 2011. Temperature-independent Curvature Sensor using FBG Cladding Modes based on a Core Misaligned Splice. *IEEE Photonics Technology Letters*, Volume 23(12), pp. 804–806

Hall, R.N., Fenner G.E., Kingsley, J.D., Soltys, T.J., Carlson, R.O., 1962. Coherent Light Emission From GaAs Junctions. *Phys. Rev*. Lett., Volume 9, pp. 366–269

Holonyak, N. Jr., Bevacqua, S.F., 1962. Coherent (visible) Light Emission from $Ga(As_{1-x}P_x)$ Junctions. *Appl. Phys. Lett*., Volume 1(4), pp. 82–83

Kao, K.C., Hockham, G.A., 1966. Dielectric-fibre Surface Waveguides for Optical Frequencies. In: *Proceedings of the IEEE,* Volume 133(3) pp. 191–198

Kim, Y.H., Kim, M.J., Rho, B.S., Park, M.S., Jang, J.H., Lee, B.H., 2011. Ultra Sensitive Fiber-optic Hydrogen Sensor based on High Order Cladding Mode. *IEEE Sensors Journal*, Volume11 (6), pp. 1423–1426

Lieberman, R.A, Blyler, L.L., Cohen, L.G., 1990. A Distributed Fiber Optic Sensor based on Cladding Fluorescence. *Journal of Lightwave Technology*, Volume 8(2), pp. 212–219

Maiman, T., 1960. Stimulated Optical Radiation in Ruby. *Nature*, Volume 187(4736), pp. 493–494

Priambodo, P.S., Raharjo, S., Witjaksono, G., Hartanto, D., XXXX. Fiber Optic Ring Resonator Sensor Detection Technique based on Spectra Intensity Integration. *Makara J. Technol*., Volume 19(1), pp. 25–30

Raharjo, S., Priambodo, P.S., Hartanto, D., Sudibyo, H., 2014. Optimalization of Cross- and Direct- Type of Fiber Optic Ring Resonator (FORR) with Coupling Coefficient (κ) variation. *International Journal of Optics and Applications*, Volume 4(4), pp. 101–109

Saleh, B.E.A., Teich, M.C., 1991. Fundamentals of Photonics. A Wiley-Interscience Publication, John Wiley and Sons, Inc., Ch. 7 "*Optical Coupling in Waveguides*," pp. 264–267

Schawlow, A.L., Townes, C.H., 1958. Infrared and Optical Masers. *Phys. Rev*., Volume 112(6), pp. 1940–1949

Stupar, D.Z., Bajie, J.S., Manojlovie, L.M., Slankamenac M.P., Joza, A.V., Zivanov, M.B., 2012. Wearable Low-cost System for Human Joint Movements Monitoring based on Fiber-optic Curvature Sensor. *IEEE Sensors Journal*, Volume 12(12), pp. 3424–3431

Zhang, Y., Xue, L., Wang, T., Yang, L., Zhu, B., Zhang, Q., 2014. High Performance Temperature Sensing of Single Mode-Multimode-Single Mode Fiber with Thermo-Optic Polymer as Cladding of Multimode Fiber Segment. *IEEE Sensors Journal*, Volume14(4), pp. 1143–1147

Zhou, W., Zhou, Y., Dong, X., Shao, L.Y., Cheng, J., Albert, J., 2012. Fiber-optic Curvature Sensor based on Cladding-Mode Bragg Grating Excited by Fiber Multimode Interferometer. *IEEE Photonics Journal*, Volume 4(3), pp. 1051–1057